

## Analysis of Hagen-Poiseuille Flow Using SPH

**Moon Wonjoo**

*Research Team of Design for Structural Integrity, Division of Electrical and Mechanical Engineering,  
Yonsei University, 134 Shinchon-dong, Seodaemun-gu, Seoul 120-749, Korea*

**You Sukbeom**

*Product Design Team, Samsung SDI Co., Ltd, 575, Shin-dong, Paldal-gu, Suwon,  
Kyunggi-do 442-391, Korea*

**Min Oakkey\***

*Division of Electrical and Mechanical Engineering, Yonsei University,  
134 Shinchon-dong, Seodaemun-gu, Seoul 120-749, Korea*

This paper shows how to formulate the transient analysis of 2-dimensional Hagen-Poiseuille flow using smoothed particle hydrodynamics (SPH). Treatments of viscosity, particle approximation and boundary conditions are explained. Numerical tests are calculated to examine effects caused by the number of particles, the number of particles per smoothing length, artificial viscosity and time increments for 2-dimensional Hagen-Poiseuille flow. Artificial viscosity for reducing the numerical instability directly affects the velocity of the flow, though effects of the other parameters do not produce as much effect as artificial viscosity. Numerical solutions using SPH show close agreement with the exact ones for the model flow, but SPH parameter must be chosen carefully. Numerical solutions indicate that SPH is also an effective method for the analysis of 2-dimensional Hagen-Poiseuille flow.

**Key Words :** SPH (Smoothed Particle Hydrodynamics), Kernel Function, Smoothing Length, Imaginary Particle, Particle Approximation, Artificial Viscosity

### 1. Introduction

Smoothed Particle Hydrodynamics (SPH) is a pure Lagrangian hydrocode and gridless method, which uses particles instead of grids or elements. This method has been suggested as an alternative to conventional grid-based hydrocodes which have some drawbacks such as the grid tangling in large deformation by Lagrangian technique and the increase of computational cost caused in void formulation by Eulerian technique. To overcome the drawbacks of conventional grid-based hydrocodes, SPH was introduced by Lucy (1977)

\* Corresponding Author,

**E-mail :** minokey@yonsei.ac.kr

**TEL :** +82-2-2123-2817; **FAX :** +82-2-362-2736

Division of Electrical and Mechanical Engineering,  
Yonsei University, 134 shinchon-dong, Seodaemun-gu,  
Seoul, 120-749, Korea (Manuscript Received August  
10, 2001; Revised December 27, 2001)

for an application in astrophysics and has been developed by researchers in various fields (Min et al., 1996; Petschek and Liversky, 1993; Bonet and Kulasegram, 2000; Randles and Liversky, 1996). In addition, SPH has been applied successfully to a wide range of problems. The basic concept and formulation were reviewed by Monaghan and Gingold (1983). An application of SPH to an analysis of low Reynolds number flows was performed by Takeda et al. (1994) and Morris et al. (1997). Takeda et al. have solved the compressible gases with Reynolds number down to five using SPH. They analyzed the flow in a duct using 3-dimensional particle allocation and compared their results with FDM solutions. Morris et al. have analyzed low Reynolds number ( $Re \leq 1$ ) incompressible flow between infinite plates. Their results were favorable with exact solutions, but they did not model the flow in a duct using SPH. Morris (2000) simulated two-

phase flows including surface tension using SPH. He suggested several possible implementations of surface tension force. Likewise, many applications to the fields of environmental, mechanical, and petroleum engineering involve the slow viscous flow through the filters, substrates, and porous materials. The advantages of SPH are that no hard calculations for generation or rezoning of grids are necessary and no special treatments are necessary for multi-component fluid (Monaghan and Kocharyan, 1994).

In this paper, the basic equations of SPH are briefly reviewed and the transformed formulations of the equations in cylindrical coordinates are presented. Also, how to formulate the transient analysis of Hagen-Poiseuille flow in 2-D cylindrical flow with low Reynolds number is shown using smoothed particle Hydrodynamics (SPH). SPH solution of Hagen-Poiseuille flow has been compared with the exact solution. Additionally, the analyses of effects caused by the number of particles, the number of particles per smoothing length (NPH), artificial viscosity and time increments for the flow are performed.

## 2. SPH Formulation in Cylindrical Coordinates

Formulations of SPH in cylindrical coordinates for functions and differential equations were given by Min et al. (2000), and the governing equations for the analysis of Hagen-Poiseuille flow are the continuity equation and the momentum conservation equation (Navier Stokes equation). The general representations of those governing equations are reviewed and the transformed formulations in cylindrical coordinates are presented.

### 2.1 SPH form of the governing equations

The foundation of SPH method is an interpolation theory. The governing equations, in the form of partial differential equations, are transformed into the integral through the use of an interpolation function that gives the kernel estimate of field variables at a point. Computationally, the integrals are evaluated as sums

over neighboring points. The basic form of SPH approximation is given as follows (Liversky et al., 1993)

$$f(\mathbf{x})_i = \sum_{j=1}^n \frac{m_j}{\rho_j} f(\mathbf{x}_j) W(\mathbf{x}_i - \mathbf{x}_j, h) \quad (1)$$

where  $W(\mathbf{x} - \mathbf{x}', h)$  means kernel function. The function at particle  $i$  is determined from the interpolation of function at neighboring particle  $j$  by the kernel function where,  $m$  denotes mass and  $\rho$  denotes density. There are several types of kernel function such as Gaussian function, exponential function, and Cubic B-spline, etc (Liversky et al., 1993). In this paper, the Gaussian function is adopted as the kernel function in cylindrical coordinates.

The governing equations of Hagen-Poiseuille flow in 2-D consist of the continuity equation and the momentum conservation equation. Applying the SPH approximation to the governing equations, the following equations in Cartesian coordinates are obtained

$$\left(\frac{d\rho}{dt}\right)_i = \left(-\rho \frac{\partial U^a}{\partial x^a}\right)_i = -\rho \sum \frac{m_j}{\rho_j} (U_j^a - U_i^a) W_{i,j} \quad (2)$$

$$\left(\frac{dU^a}{dt}\right)_i = \left(-\rho \frac{\partial \sigma^{ab}}{\partial x^b}\right)_i = -\sum m_j \left(\frac{\sigma_i^{ab}}{\rho_i^2} + \frac{\sigma_j^{ab}}{\rho_j^2}\right) W_{i,j} \quad (3)$$

$$\sigma^{ab} = p \delta^{ab} - 2\rho\nu \left(\dot{\epsilon}^{ab} - \frac{1}{3} \delta^{ab} \dot{\epsilon}^{\gamma\gamma}\right) \quad (4)$$

where  $U$ ,  $t$ ,  $\nu$ ,  $x$ ,  $\dot{\epsilon}$ , and  $\sigma$  are velocity, time, dynamic viscosity, position vector, strain rate tensor and total stress, respectively. Subscripts  $i$  and  $j$  denote the indices of particles, while superscripts  $a$  and  $b$  are tensor notations which represent direction in space.  $W_{i,j}$  means the derivative of kernel function  $W_i$  of particle  $i$  with respect to coordinate  $x^a$ . These SPH forms show that the variables at particle  $i$  are influenced by the variables at particle  $j$ .

For the most cylindrical problems, axisymmetry is taken into account and the equations in Cartesian coordinates are transformed into those in cylindrical coordinates. The stress components in the governing equations in Cartesian coordinates  $x$ ,  $y$ , and  $z$  must be transformed into those in cylindrical coordinates  $s_r$ ,  $\theta$ , and  $z$ . For transforming into the cylindrical coordinates, the contravariant tensor transformation is employed

as follows

$$\sigma^{\alpha\beta} = a_r^\alpha a_s^\beta \sigma^{rs} \quad (5)$$

where  $a_r^\alpha$  means the direction cosine. The momentum conservation in two cylindrical coordinates  $s_r$  and  $z$  can be yielded by applying the tensor transformation for stresses in Eq. (5) and the symmetry of cylindrical coordinates to the momentum conservation equation in Cartesian coordinates. The momentum equations in cylindrical coordinates can be expressed as

$$\begin{aligned} \left(\frac{dU^r}{dt}\right)_i &= \frac{2}{h^2} \sum_j m_j W_c \left\{ \frac{\sigma_j^{rr}}{\rho_j^2} \left( r_i \frac{I_0 + I_2}{2I_0} - r_j \frac{I_1}{I_0} \right) \right. \\ &\quad + \frac{\sigma_j^{\theta\theta}}{\rho_j^2} r_i \frac{I_0 - I_2}{2I_0} + \frac{\sigma_j^{rz}}{\rho_j^2} (z_i - z_j) \frac{I_1}{I_0} \\ &\quad \left. + \frac{\sigma_i^{rr}}{\rho_i^2} \left( r_i - r_j \frac{I_1}{I_0} \right) + \frac{\sigma_i^{rz}}{\rho_i^2} (z_i - z_j) \right\} \end{aligned} \quad (6)$$

$$\begin{aligned} \left(\frac{dU^z}{dt}\right)_i &= \frac{2}{h^2} \sum_j m_j W_c \left\{ \frac{\sigma_j^{rz}}{\rho_j^2} \left( r_i \frac{I_1}{I_0} - r_j \right) \right. \\ &\quad \left. + \frac{\sigma_j^{zz}}{\rho_j^2} (z_i - z_j) + \frac{\sigma_i^{rz}}{\rho_i^2} \left( r_i - r_j \frac{I_1}{I_0} \right) + \frac{\sigma_i^{zz}}{\rho_i^2} (z_i - z_j) \right\} \end{aligned} \quad (7)$$

where  $I_n$  is the modified Bessel's function of  $n^{\text{th}}$  order and  $W_c$  is a 2-dimensional cylindrical kernel function given as

$$W_c(\xi) = \frac{1}{2\pi} \int_0^{2\pi} G e^{-\xi} e^{\xi \cos \theta} d\theta = G e^{-\xi} I_0(\xi) \quad (8)$$

where  $\xi$  and  $G$  are given by the smoothing length  $h$  and the position of two particles  $r_i$  and  $r_j$  as

$$\xi = \frac{2r_i r_j}{h^2} \quad (9)$$

$$G = \frac{1}{\pi^{3/2} h^3} e^{-((r_i - r_j)^2 + (z_i - z_j)^2)/h^2} \quad (10)$$

The transformation of the other governing equation is performed as above. The continuity equation of Hagen-Poiseuille flow in cylindrical coordinates is transformed into as follows

$$\begin{aligned} \left(\frac{d\rho}{dt}\right)_i &= -\rho_i \frac{2}{h^2} \sum_j \frac{m_j}{\rho_j} W_c \left\{ U_i^r \left( r_i - r_j \frac{I_1}{I_0} \right) \right. \\ &\quad \left. + (U_i^z - U_j^z) (z_i - z_j) - U_j^r \left( r_i \frac{I_1}{I_0} - r_j \right) \right\} \end{aligned} \quad (11)$$

## 2.2 Artificial viscosity

In the analysis of this model, numerical oscillation occurs at the wall, which brings about the divergence of solution. An artificial viscosity is introduced in the momentum equation in order to reduce numerical oscillation. Monaghan and

Gingold (1983) suggested an artificial viscosity  $\Pi_{ij}$  when two particles  $i$  and  $j$  approach each other as

$$\Pi_{ij} = \begin{cases} \frac{-\alpha \bar{c}_{ij} \mu_{ij} + \beta \mu_{ij}^2}{\bar{\rho}_{ij}} & \text{for } \mathbf{U}_{ij} \cdot \mathbf{x}_{ij} < 0 \\ 0 & \text{for } \mathbf{U}_{ij} \cdot \mathbf{x}_{ij} > 0 \end{cases} \quad (12)$$

where  $\bar{c}_{ij}$  and  $\bar{\rho}_{ij}$  are the average impact wave velocity and the average density at particles  $i$  and  $j$ , respectively. The parameter  $\alpha$  is equivalent to a combined Navier-Stokes shear and bulk viscosity and can be replaced by a proper Navier-Stokes viscosity, while the parameter  $\beta$  is similar to a Von Neumann-Richtmyer viscosity and is needed to prevent penetration in high Mach shocks. The simulation without artificial viscosity makes results of flow diverged. The parameter  $\mu_{ij}$  is expressed in terms of the displacement difference and velocity difference of two particles as

$$\mu_{ij} = \frac{h \mathbf{U}_{ij} \cdot \mathbf{x}_{ij}}{\mathbf{x}_{ij} + \varepsilon h^2} \quad (13)$$

and  $\mu_{ij}$  in Cartesian coordinates can be transformed into that in cylindrical coordinates as

$$\mu_{ij} = \frac{h \left\{ r_{ij} U_{ij}^r + z_{ij} U_{ij}^z + (r_i U_j^r + r_j U_i^r) \left( 1 - \frac{I_1}{I_0} \right) \right\}}{\left\{ r_{ij}^2 + z_{ij}^2 + \varepsilon h^2 + 2r_i r_j \left( 1 - \frac{I_1}{I_0} \right) \right\}} \quad (14)$$

where  $r_{ij} = r_i - r_j$ ,  $z_{ij} = z_i - z_j$  and  $U_{ij} = U_i - U_j$ .

The artificial viscosity  $\Pi_{ij}$  is applied to the stress terms in momentum equations of Hagen-Poiseuille flow in cylindrical coordinates.

## 2.3 Boundary conditions of the model flow

To a realistic model flow at lower Reynolds numbers, no-slip boundary conditions are needed on the wall. We used "imaginary particle" of Libersky et al. (1993) for no-slip boundary conditions. Imaginary particles do not calculate their physical values from the neighboring particles, but they do affect calculation of neighboring real particles on the wall.

Use of imaginary particles in the simulation for boundary conditions is shown in Fig. 1. Imaginary particles can be created by reflecting real particles across the boundary with the same magnitude and opposite direction velocities to those of particles within  $3h$  from the boundary. Veloci-

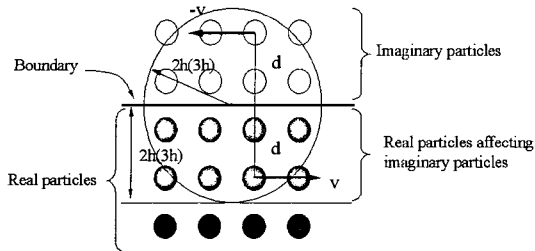


**Fig. 1** Construction of imaginary particles for no-slip boundary condition

ties in the boundary thus become zero in the case of particles approximation.

### 3. Simulation of Hagen-Poiseuille Flow and Error Estimate

The viscous flow in a duct is a practical engineering problem. To exemplify the SPH formulation, transient Newtonian fluid with the constant viscous coefficient through a circular duct has been simulated. If we take a flow in an axis direction, only  $z$ -direction flow exists because of axisymmetry of the flow.

#### 3.1 Exact solution

Hagen-Poiseuille flow is rest at initial and is driven by an applied acceleration term due to the pressure gradient parallel to the  $z$ -axis for  $t \geq 0$ . No-slip boundary condition is needed on the circular duct wall. When Hagen-Poiseuille flow conditions are applied to momentum equation in the cylindrical coordinate, Eq. (3) becomes as follows

$$\frac{dU^z}{dt} = \nu \frac{1}{r} \frac{\partial}{\partial r} \left( r \frac{\partial U^z}{\partial r} \right) + A^z \quad (15)$$

$$A^z = -\frac{1}{\rho} \frac{\partial p}{\partial z} \quad (16)$$

where,  $A^z$  is an acceleration term due to the pressure gradient to the  $z$ -direction. Using Bessel function and Fourier series, above partial differential equation can be solved. The exact solution is written as follows

$$U^z(r, t) = \frac{A^z}{4\nu} R^2 \left( 1 - \frac{r^2}{R^2} \right) + \sum_{m=1}^{\infty} a_m e^{-\lambda_m t} J_0 \left( \frac{\alpha_m}{R} r \right) \quad (17)$$

**Table 1** Analysis conditions for Hagen-Poiseuille flow

Radius ( $R$ )	$10^{-3} m$
Density ( $\rho$ )	$10^3 kg/m^3$
Dynamic viscosity ( $\nu$ )	$10^{-6} m^2/s$
Acceleration ( $A^z$ )	$10^{-4} m/s^2$

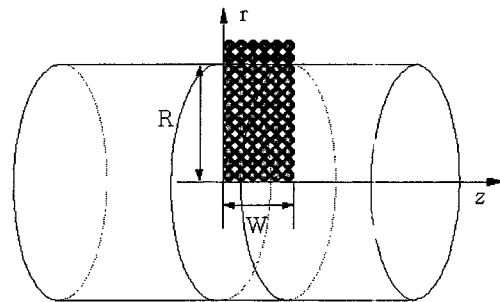


**Fig. 2** Allocation of particles in a circular duct

$$a_m = \frac{2}{R^2 J_1^2(\alpha_m)} \int_0^R \left\{ -r \frac{A^z}{4\nu} R^2 \left( 1 - \frac{r^2}{R^2} \right) J_0 \left( \frac{\alpha_m}{R} r \right) \right\} dr \quad m=1, 2, 3, \dots \quad (18)$$

where,  $J_0$  is Bessel function of the first kind of order 0,  $\alpha_m$  are sequential series solutions satisfying  $J(\alpha_m) = 0$ ,  $R$  is radius of circular duct and  $\nu$  is dynamic viscosity. In Eq. (17), the first term in the right-hand side represents a steady state flow profile while the second term indicates transient velocity profile. The analysis conditions for the model are listed in Table 1.

#### 3.2 Numerical analysis

For SPH analysis, the particles in 2-dimensional are allocated as shown in Fig. 2. The problem domain is filled with particles in rectangular allocation. Particles on the outside of a circular duct are imaginary particles to meet a no-slip boundary condition. The allocation of particles is axisymmetry. In Fig. 2,  $R$  and  $W$  mean the radius of circular duct and the width in the  $z$ -direction, respectively.

Effects by the number of particles, the number of particles per smoothing length (NPH), artificial viscosity and time increments for the flow have been analyzed. Basic analysis conditions for simulations of the model flow are listed in Table

**Table 2** Analysis conditions for Hagen-Poiseuille flow by SPH

$R \times W$ (number of particles)	40 × 8
NPH (number of particles per smoothing length)	1
Artificial viscosity coefficients ( $\alpha, \beta$ )	0.5, 0.0
Time increment ( $\delta t$ )	100 $\mu$ sec

2. The maximum velocity of the numerical solution (SPH) is compared with the exact one and the error by the error equation in Eq. (19) is estimated.

$$Error_{t_n} = \frac{(U_{max}^z)_{SPH,t_n} - (U_{max}^z)_{Exact,t_n}}{(U_{max}^z)_{Exact,t_n}} \quad (19)$$

where,  $U_{max}^z$  is maximum velocity in z-direction and  $t_n$  is sequential times from 40ms to 400 ms. The increment of flow velocity is radically reduced to 95% of fully developed velocity in 400 ms.

### 3.2.1 Effect of the number of particle

More accurate solutions may be expected by increasing the number of particles. The computation time would increase if the number of particles was to be increased. Furthermore, the increment of the number of particles requires in decrement of the time increment for numerical stability. The decrease of the time increment makes a radical increase of the computation time. For efficient solutions, the optimized number of particles should be selected without causing the large error.

To find the optimum number of particles, numerical tests are performed for the model flow by using various numbers of particles  $R$  (length of radius)  $\times W$  (width in the z-directions) such as  $20 \times 4$ ,  $30 \times 6$ ,  $40 \times 8$ , and  $50 \times 10$ . Other parameters are used as the values listed in Table 2. The results in Fig. 3 show that the increase of number of particles somewhat made flow velocity increased. However, the effect of the number of particles slightly affects the solution directly.

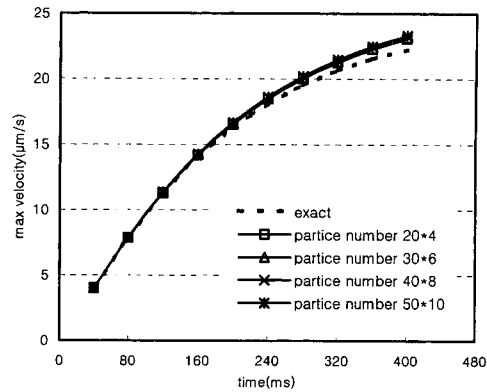


**Fig. 3** Maximum velocities in Hagen-Poiseuille flow in terms of the number of particles in SPH

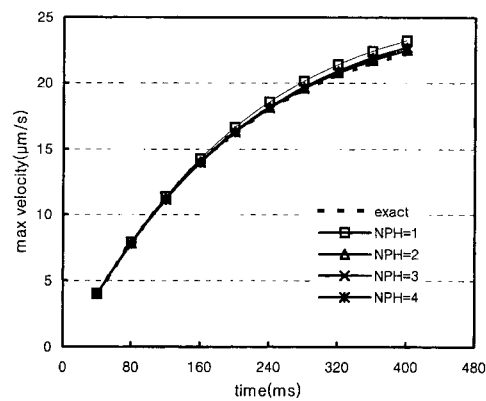


**Fig. 4** Maximum velocities in Hagen-Poiseuille flow in terms of NPH

### 3.2.2 Effect of NPH

NPH (number of particles per smoothing length) represents the number of particles within the smoothing length in arbitrary directions. When the initial distance between particles is fixed, NPH determines the smoothing length of kernel by multiplying each particle distance. Increase in NPH provides with providing a wider region to approximate particles, which makes numerical instability reduced. In that case, the difference of physical values among the particles could be reduced, and numerical results are more or less equalized. As NPH increases, the number of neighboring particles which should be calculated per particle tends to be increased. The increase of the number of neighboring particles

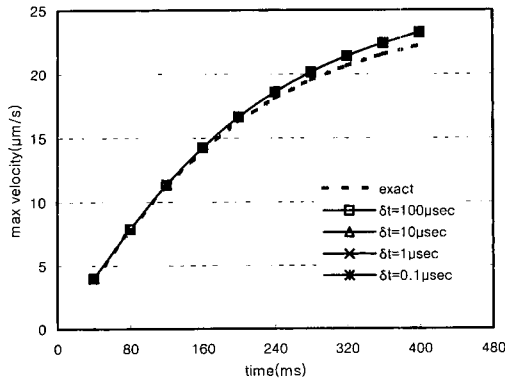


Fig. 5 Maximum velocities in Hagen-Poiseuille flow in terms of the time increment

causes the increase of simulation time. The numerical tests for the model flow are performed using parameters in Table 2 and shown in Fig. 4. NPH is changed for 1, 2, 3, and 4 in turn. In the results of numerical tests, the increase of NPH makes flow speed more or less reduced, however effect of NPH is shown not to greatly affect the solution.

### 3.2.3 Effect of the time increment

As the SPH formulation calculates physical values at the arbitrary time based on finite difference method, the time increment ( $\delta t$ ) affects the error of solution directly. As time increment is related to numerical stability in numerical integration, an excessive time increment may result in numerical instability. On the other hand, the small time increment may have an advantage in numerical stability. The small time increment, however, prolongs the calculation time with increasing the number of iterations. An optimized time increment should be selected. The flow is simulated using the parameters in Table 2 except for the time increment and the choice of the time increment is 0.1, 1, 10, 100  $\mu$ sec in turn. In spite of increasing ten times of the time increment, the results of calculation are hardly affected as shown in Fig. 5. But the time increment directly affects the analysis time. Therefore, the selection of the time increment is important for the analysis efficiency.

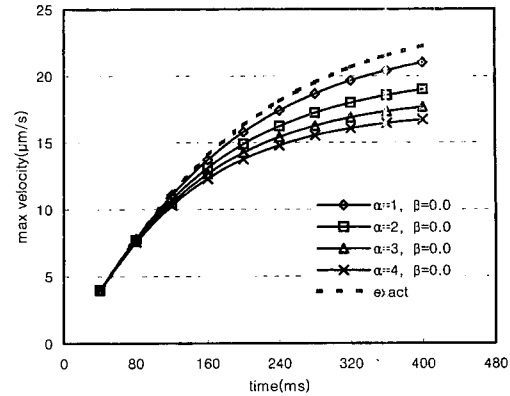


Fig. 6 Effect of parameter  $\alpha$  in artificial viscosity in Hagen-Poiseuille flow

### 3.2.4 Effect of artificial viscosity

Even though the artificial viscosity in SPH prevents numerical instability on boundaries where physical values change radically, the artificial force added in the momentum term causes viscous(damping) force in proportional to the magnitude of artificial force. In this section, the effect of artificial viscosity which consists of  $\alpha$  and  $\beta$  terms in Eq. (12) is analyzed. Effect and error of the term in artificial viscosity are shown in Fig. 7. The model flow is simulated by changing  $\alpha=1, 2, 3, 4$  in turn with fixed  $\beta=0.0$ . As can be seen in Fig. 6, the parameter  $\alpha$  has an effect on the flow results. In case of  $\alpha=0.0$ , results could not be obtained because of the divergence on the boundary. The increase of  $\alpha$  made flow speed decreased by increasing viscous(damping) force. A small  $\alpha$  greater than 0.0 and much less than 1.0 is recommended to yield a reasonable solution.

Effect of the parameter  $\beta$  term in artificial viscosity is shown in Fig. 7. Numerical simulation with  $\alpha=0.0$  makes numerical procedure unstable. Hence, the model flow is simulated by changing  $\beta=1, 2, 3, 4$  in turn with fixed  $\alpha=0.5$ . From these experiments in Fig. 7, it is understood that the parameter  $\beta$  has little effect on the solutions. As mentioned in Sec. 2.2, the parameter  $\beta$  in the artificial viscosity plays a part in preventing penetration in high Mach shock. Since this simulation model has a low speed, the parameter  $\beta$  is considered to be little influence on the solution. The  $\beta \mu_y^2$  term in artificial viscosity is

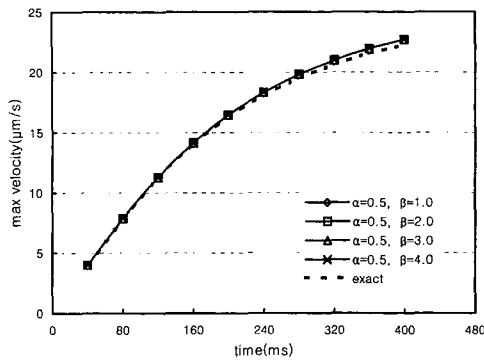


Fig. 7 Effect of parameter  $\beta$  in artificial viscosity in Hagen-Poiseuille flow

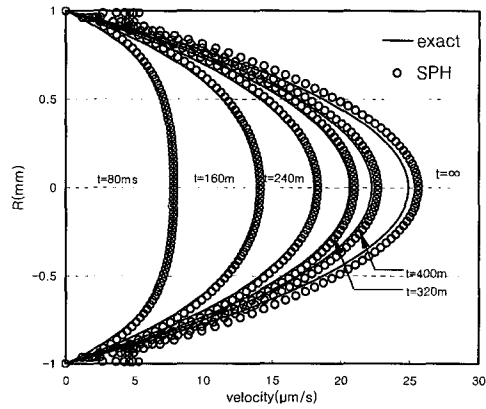


Fig. 9 Comparison of SPH and exact solutions for Hagen-Poiseuille flow

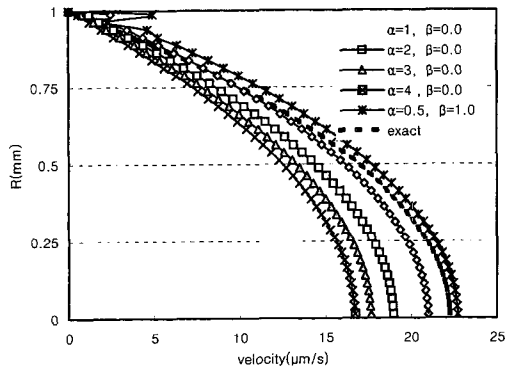


Fig. 8 Oscillation on the boundary in Hagen-Poiseuille flow

almost zero because the estimated  $\mu_{ij}$  is very small. The term including  $\alpha$  plays a part in reducing numerical instability and operates like a real viscous. The magnitude of  $\alpha C_{ij} \mu_{ij}$  directly influences on the flow.

Fluctuation on the boundary for various  $\alpha$  is shown in Fig. 8. Because of the divergence on the boundary, results of  $\alpha=0.5$  and  $\beta=1.0$  are presented instead of results of  $\alpha=0.0$  and  $\beta=0.0$ . This fluctuation is shown to be decreased by the increment of the parameter of the artificial viscosity. The reason of such a phenomenon has not been proved yet. Further improvements for the implement of the boundary conditions to reduce this fluctuation need to be taken.

Speed profiles of transient flow are shown in Fig. 9, where the solid line represents exact solutions and the dotted profile represents solutions of SPH simulation with respect to time.

The SPH transient solutions using parameters in Table 2 are very similar to the exact solutions. When analysis time reaches 1 sec, the velocity increment is less than 0.01%. With this reason, it can be assumed that velocity profiles are almost fully developed. The results show that the error increase as time increases is less than 2% when fully developed.

#### 4. Conclusions

The Hagen-Poiseuille flow in 2-dimensional has been analyzed by using Smoothed Particle Hydrodynamics (SPH). For SPH analysis, the particles are arranged in 2-dimension to reduce the computation time and numerical solutions are compared with the exact solution. Analysis of effects caused by the number of particles, the number of particles per smoothing length (NPH), artificial viscosity and time increments for the flow are performed. The results of numerical tests show that the effects of the number of particles, the number of particles per smoothing length and time increments are very small. As for artificial viscosity of Monaghan & Gingold for reducing numerical instability, the parameter  $\alpha$  affects dominantly on the solutions. From the analysis of effects of principal parameters, the simulation results of Hagen-Poiseuille flow by using SPH are very similar to the exact solution if appropriate parameters were used.

From the above results, it is convinced that

SPH is also an effective method for axisymmetric 2-dimensional analysis of Hagen-Poiseuille transient flow.

### References

- Bonet, J. and Kulasegram, S., 2000, "Correction and Stabilization of Smooth Particle Hydrodynamics Methods with Applications in Metal Forming Simulations," *Int. J. Numer. Meth. Engng.*, Vol. 47, pp. 1189~1214.
- Libersky, L. D., Petschek, A. G., Carney, T. C., Hipp, J. R. and Allahdadi, F. A., 1993, "High Strain Lagrangian Hydrodynamics: A Three-Dimensional Response," *J. Comput. Phys.*, Vol. 109, pp. 67~75.
- Lucy, L. B., 1997, "A Numerical Approach to the Testing of the Fission Hypothesis," *Astron. J.*, Vol. 82, pp. 1013~1020.
- Min, O., Lee, J., Kim, K., Park, H., 1996, "An Application of Smoothed Particle Hydrodynamics in Analysis of Dynamic Elasto-Plastic Deformation," *Proc. of 2nd ISIE '96*, pp. 392~397.
- Min, O., Lee, J., Kim, K. and Lee, S., 2000, "A Contact Algorithm in the Low Velocity Impact Simulation with SPH," *KSME Int. J.*, Vol. 114, pp. 705~714.
- Monaghan, J. J. and Gingold, R. A., 1983, "Shock Simulation by the Particle method SPH," *J. Comput. Phys.*, Vol. 52, pp. 374~389.
- Monaghan, J. J. and Kocharyan, A., 1994, "SPH simulation of multi-phase flow," *J. Comput. Phys.*, Vol. 87, pp. 225~235.
- Morris, J. P., Fox, P. J. and Yi, Z., 1997, "Modeling Low Reynolds Number Incompressible Flow Using SPH," *J. Comput. Phys.*, Vol. 136, pp. 214~226.
- Morris, J. P., 2000, "Simulating Surface Tension with Smoothed Particle Hydrodynamics," *Int. J. Numer. Meth. Fluids.*, Vol. 33, pp. 333~353.
- Petschek, A. G. and Libersky, L. D., 1993, "Cylindrical Smoothed Particle Hydrodynamics," *J. Comput. Phys.*, Vol. 109, pp. 76~83.
- Randles, P. W. and Libersky, L. D., 1996, "Smoothed Particle Hydrodynamics: Some Recent Improvements and Applications," *Comput. Methods Appl. Mech. Engrg.*, Vol. 139, pp. 375~408.
- Takeda, H., Miyama, S. M. and Sekiya, M., 1994, "Numerical Simulation of Viscous Flow By Smoothed Particle Hydrodynamics," *Prog. Theor. Phys.*, Vol. 92, pp. 939~960.